MRS Advances © 2018 Materials Research Society
DOI: 10.1557/adv.2018.308

Solution Based Synthesis of Cs_4PbBr_6 Perovskite Particles with High Luminescence and Stability

Brian Billstrand[1], Kaifu Bian[1], Casey Karler[1], Dongmei Ye[1], Austin Hwang[1], Hongyou Fan[1,2,*]

[1]Sandia National Laboratories, Advanced Materials Laboratory, Albuquerque, New Mexico, 87106, United States;

[2]The University of New Mexico Center for Micro-Engineered Materials, Department of Chemical and Biological Engineering, Albuquerque, New Mexico 8713, United States

ABSTRACT

Low dimensional lead halide perovskite particles are of tremendous interest due to their size-tunable band gaps, low exciton binding energy, high absorption coefficients, outstanding quantum and photovoltaic efficiencies. Herein we report a new solution-based synthesis of stabilized Cs_4PbBr_6 *perovskite particles with high luminescence. This method requires only mild conditions and produces colloidal particles that are ideal for highly efficient solution-based device fabrications. The synthesized microstructures not only display outstanding luminescence quantum yield but also long term stability in atmospheric conditions. Partial halide substitutions were also demonstrated to extend photoluminescence spectra of the perovskite particles. This convenient synthesis and optical tunability of* Cs_4PbBr_6 *perovskite particles will be advantageous for future applications of optoelectronic advices.*

INTRODUCTION

Low dimensional organic and inorganic lead halide perovskite particles are of tremendous interest due to their size-tunable band gaps, low exciton binding energy, high absorption coefficients,[1] outstanding luminescence and photovoltaic efficiencies.[2] To overcome the atmospheric vulnerability of traditional methylammonium based devices, recent research trend has focused on materials utilizing cesium cation in combination with a wide variety of long chain ammonium ligands to improve environmental stability and tune the dimension and band gap of perovskite structures.[3-7] Perovskite produced by these methods generally have ABX_3, AB_2X_5, and A_4BX_6 structures in layers separated by alkylammonium ligands that interact via van der Waals forces. Here A represents an alkaline metal cation such as Cs^+, B represents a cation such as Pb^{2+} or Sn^{2+}, and X represents a halide ion such as I^-, Br^-, or Cl^-. These structures displayed high photoluminescence quantum yields (PLQY) of 20 - 90%.[8-10]

As a major challenge, most perovskite materials suffer from very limited atmospheric stability. It has previously been addressed through the efforts including contact passivation and polymeric coatings.[4, 11, 12] This work has focused on synthesizing uniform perovskite particles with a variety of hydrophobic tetraalkylammonium ligands to improve stability of inorganic perovskite materials while provide high quantum efficiency simultaneously. As a result, a solution-based synthesis of cesium lead bromide particles was developed. Compared with previously reported hot injection methods which require high temperature, vacuum, inert environment and high-boiling point solvents,[3, 10, 13-16] this inexpensive synthesis was carried out under mild conditions: room temperature, ambient air and with easy-to-remove solvents.[5] The product particles displayed high quantum yield and enhanced stability. In addition they form homogenous colloidal suspensions in common solvents, desirable for highly efficient solution-based processing and device fabrications.

EXPERIMENT

Materials

All chemicals were purchased from Sigma Aldrich and used without further purification. Lead bromide (PbBr, 99%), cesium bromide (CsBr, 99%), tetramethylammonium bromide (TMABr, 99%), tetraethylammonium bromide (TEABr, 99%), tetraethylammonium chloride (TEACl, 99%), tetraethylammonium iodide (TEAI, 99%), tetrabutylammonium bromide (TBABr, 99%), tetraoctylammonium bromide (TOABr, 99%), dimethylformamide (DMF, 99%), toluene (Tol., 99%).

Preparation of Cs_4PbBr_6 and Halide Substitutions

In a typical synthesis 0.1 mmol of TEABr, TBABr or TOABr was added to a vial and mixed with 5 mL of DMF. Next PbBr and CsBr were dissolved consecutively in the solution using a 1:2:1 (PbBr: TEABr/TBABr/TOABr: CsBr) molar ratio. This solution was then added to a 20 mL glass vial and sonicated. Sonication was performed using a 125 W Qsonica sonicator at a frequency of 20 kHz at 60% amplitude. The reaction could be also performed with simple stirring. Quickly after starting sonication 5 mL of toluene was injected and the solution turned cloudy and white. The suspension was then allowed to be sonicated for an additional 20 minutes to ensure completion of the reaction. This was signaled by the color change to yellow. Next, the raw product was centrifuged for 10 minutes at 9500 rpm, washed with toluene and then dispersed in toluene for storage and characterization. It is worth mentioning that the hygroscopic tetra-ammonium precursors need to be completely free of humidity since hydrated precursors will significantly reduce PLQY of the final perovskite products. Anhydrous solvents and a dry environment are also desired. Halide substitutions were performed by replacing TEABr with 0.1 mmol of either TEAI or TEACl in the initial precursor solution using the 1:2:1 PbBr:TEA:CsBr ratio. Then the synthesis was carried out in the same fashion.

Characterization Methods

SEM images were taken using a Hitachi S-5200 scanning electron microscope operating at 2.0kV and 15 μA. SEM samples were prepared by drop-casting peroskite particle suspensions in toluene onto a diced and cleaned silicon wafer and dried in atmosphere. XRD was performed using a PANalytical X'Pert PRO operating at 45kv and

40mA. XRD samples were prepared by drop-casting concentrated toluene suspension of product onto a glass microscope slide to form a thick film. PLQY measurements on solid samples deposited directly on UV quartz substrates were performed with a Horiba Fluoromax-4 Spectrofluorometer with an add-on integrating sphere. All samples were excited by monochromatic light at wavelength of 360 nm and the emission spectrum was collected between 450 and 600 nm.

RESULTS AND DISCUSSION

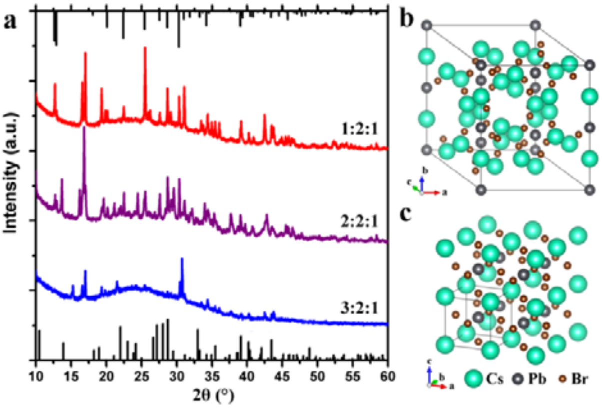

Figure 1. Structural analysis of product perovskites obtained with different precursor ratio. (a) Powder X-ray Diffraction patterns of TEA-confined materials with different precursor ratios (Pb:TEA:Cs). The theoretical XRD patterns for Cs_4PbBr_6 and $CsPbBr_3$ structures are marked on top and bottom of the chart respectively for reference. The references were calculated based on (b) Crystal structure of Cs_4PbBr_6 and (c) Crystal structure of cubic $CsPbBr_3$.

In a typical synthesis, lead bromide, tetraethylammonium (TEA) bromide and cesium bromide were dissolved in dimethylformamide (DMF). Next, this mixture was added to an equal volume of toluene while stirring or under ultrasonication. Precipitation of the perovskite particles completed in 4 hrs. The final yellow suspension was then cleaned by centrifugation and re-dispersed in toluene for characterization (See detailed synthesis and characterization methods in Supporting Information). The ratio between precursors was varied to explore crystal structure and particle morphology. Pb:TEA:Cs ratios of 1:2:1, 2:2:1, and 3:2:1 were studied. Based upon these stoichiometric ratios either $CsPbBr_3$ or $CsPb_2Br_5$ perovskite structures were expected.[9] As revealed by XRD patterns in Figure 1a, the 3:2:1 precursor ratio yielded $CsPbBr_3$ perovskite (Figure 1c). However the 1:2:1 ratio yielded a pure Cs_4PbBr_6 phases (Figure 1b) while the 2:2:1 precursor ratio showed a transition or mixture state. The Cs_4PbBr_6 crystal was indexed to have a rhombohedral lattice (space group *R-3*c) with parameters of $a = b = 13.72$ Å and $c = 17.30$ Å. This phase is believed to result from the formation of templated lead bromide ligand complexes before the incorporation of cesium into the structures, similar to the strategy of utilizing lead iodide templating organic cations to achieve pure perovskite materials.[17] This is supported by the increased intensity and blue shift from 610 nm to 560 nm of the PL peak observed in the $PbBr_2$-TEABr precursor solution in DMF comparing with $PbBr_2$-only solution. The Cs_4PbBr_6 phase is desirable for LED applications due to its larger exciton binding energies of 353 meV compared to only 19-62 neV of $CsPbBr_3$[13] as it prevents exciton dissociation into free carriers and increases luminescence efficiency.[18] Therefore, all of the syntheses discussed in the following context used 1:2:1 precursor ratio to produce Cs_4PbBr_6 perovskite.

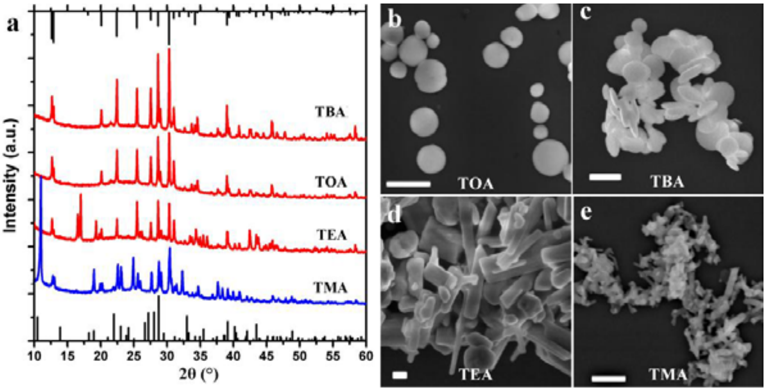

Figure 2. Comparison of crystal structure and morphology of perovskite particles synthesized with different ligand types. (a) Powder X-ray Diffraction data for the samples, calculated XRD patterns for Cs_4PbBr_6 and $CsPbBr_3$ structures are shown on the top and bottom of the chart respectively. (b-e) SEM images of perovskite particles. Scale bars are 1 µm.

To explore the ligand effect on the optical performance and stability of the perovskite particles, ligands of various alkyl chain lengths were explored including Tetraoctylammonium (TOA), tetrabutylammonium (TBA), tetraethylammonium (TEA) and tetramethylammonium (TMA). As measured by XRD (Figure 2a), all of the syntheses except the TMA-functionalized particles showed a rhombohedral R-3c crystal structure of Cs_4PbBr_6. It is also important to note the change in particle morphology (Figures 2b-2e). Crystal growth with TEA ligand resulted in rod-like structures of up to 10 µm in size, much larger compared to the platelet structures with diameters from 300 - 750 nm obtained with other ligands. The XRD patterns of the TEA particles showed a strong (202) peak ($2\theta = 17°$) indicating preferential growth in this direction and agreeing with the faceted particles. In contrast, the TOA and TBA samples lack noticeable (202) peak, consistent with the platelet particle shape. The formation of the platelet structures could be a result of crystallization hindered by the bulkier ligand molecules. The large particle size of TEA-Cs_4PbBr_6 could significantly improve charge transport within optoelectronic devices.

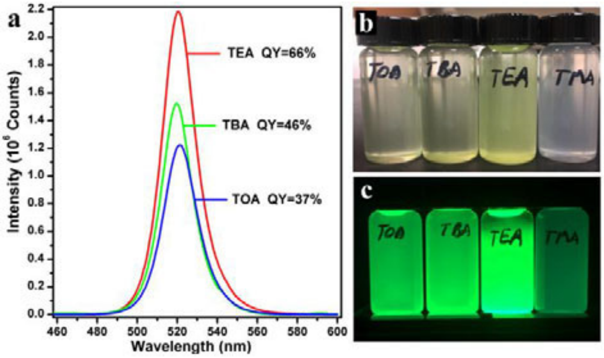

Figure 3. Photoluminance of perovskite particles functionalized by different ligands. (a) PL spectra and quantum yield from Cs_4PbBr_6 particles with TEA, TOA, and TBA ligands. (b) Cs_4PbBr_6 suspension in toluene under ambient lighting and (c) excited by UV light at 365 nm.

As presented by Figure 3a, all of the perovskite particles exhibited sharp fluorescence peaks around 520 nm with narrow width (FWHM = 9 nm). Such emission matches perfectly with the standard green according to the National Television System Committee (NTSC) making this material an excellent candidate for display applications. The highest PLQY of 66% was achieved from TEA-passivated particles. This is equal to a 15 - 20% improvement in PLQY compared to perovskite particle suspensions reported previously.[13, 14] It is also competitive with thin films of Cs_4PbBr_6 nanocrystals, which were reported to show PLQY up to 54%.[3] The structures synthesized by the TOA and TBA ligands exhibited lower quantum yield compared to the TEA structures. The different PLQY is also evidenced by comparing the photographs in Figure 3b and 3c. This is possibly the result of incomplete ligand coverage caused by sterical repulsion between the bulky tetraalkylamine ligand molecules. It is also noticed that replacing stirring with sonication further increased the PLQY by at least 15% for all ligands used due to better mixing with the best record of 75% from the TEA-passivated particles.

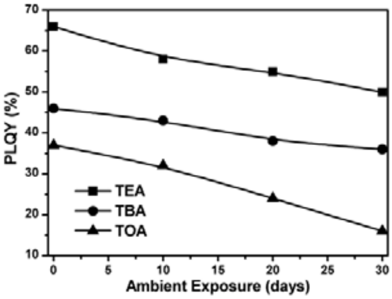

Figure 4. Degradation of of perovskite particles passivated by different ligands when exposed to atmosphere for up to 30 days.

To determine their ambient stability, the perovskite particles were deposited on glass slides and left in atmosphere for 30 days. During this period the samples' PLQY were measured every 10 days. As summarized by Figure 4, the stability of the synthesized perovskite particles improves with decreasing ligand length. A 24%, 21% and 45% reduction from the original PLQY for TEA, TBA and TOA ligands were observed respectively. In contrast, bulk Cs_4PbBr_6 perovskite was reported to lose 65% of the original quantum yield upon ambient aging for 30 days.[14] The enhanced stability was believed to result from moisture isolation by the hydrophobic alkyl chains on the ligands. The faster degradation of TOA-passivated particles was likely due to incomplete ligand coverage and partial conversion to $CsPbBr_3$ due to exposure to atmosphere, which has been previously shown to greatly reduce quantum yield.[13]

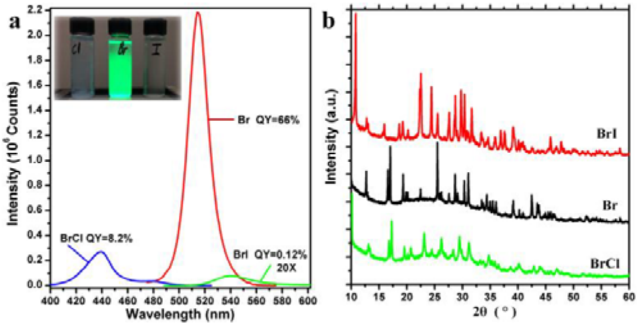

Figure 5. Partial halide substitution of perovskite particles. (a) PL spectra and quantum yield for iodide and chloride substituted particles. Inset shows toluene suspension of perovskite particles excited by UV light. (b) XRD patterns of the same samples in (a).

As a preliminary effort to tune the band gap of the perovskite particles, particle halide substitutions were performed to produce hybrid perovskite particles by replacing TEA bromide precursor by TEA chloride or TEA iodide. Larger halide anion was expected to result in lager band gaps and thus a red-shifted PL peak.[19, 20] PL spectra in Figure 5a showed that the emission peak was shifted from 520 nm for the Br only particle to 440 nm and 541 nm for the Br-Cl and Br-I hybrid structures respectively. XRD analysis in figure 5b shows a successful halide substitution indicated by the pronounced peak shifts. The iodide pattern contained unidentifiable peaks leading to the conclusion that there are additional phases and or impurities in the sample. Unfortunately the hybrid structures showed only a fraction of QY of the Br only material, possibly caused by impurities. Synthesizing a pure iodide product as an effort to improve luminescence efficiency is a subject of our further research.

CONCLUSIONS

In conclusion we report a convenient solution-based synthesis for Cs_4PbBr_6 perovskite particles. This method requires only mild conditions and can be easily scaled up. It was found that ligand of a proper molecule size and an optimized precursor ratio was important to obtain pure phase particles. These perovskite particles exhibited narrow monochromatic band gap, which was readily tuned by partial halide substitution, and PLQY up to 75% making this material an excellent candidate for light emission and display applications.

ACKNOWLEDGMENTS

This work was supported by the U.S. Department of Energy, Office of Basic Energy Sciences, Division of Materials Sciences and Engineering and Sandia's Laboratory Directed Research & Development (LDRD) program.. Sandia National Laboratories is a multimission laboratory managed and operated by National Technology and Engineering Solutions of Sandia, LLC., a wholly owned subsidiary of Honeywell International, Inc., for the U.S. Department of Energy's National Nuclear Security Administration under contract DE-NA0003525.

REFERENCES

1. L. Pazos-Outon, M. Szumilo, R. Lamboll, J. Richter, M. Crespo-Quesada, M. Abdi-Jalebi, H. Beeson, M. VruIni, M. Alsari, H. Snaith, B. Ehrler, R. Friend and F. Deschler, *Science.* **351**, 1430 (2016).
2. S. Ha, R. Su, J. Xing, Q. Zhang and X. Qiong, *Chem Science*, **8**, 2522 (2017).
3. Y. Zhang, M. Saidaminov, I. Dursun, H. Yang, B. Murali, E. Alarousu, E. Yengel, B. Alshankiti, O. Bakr and O. Mohammed, *J. Phys. Chem. Lett.* . **8**, 961 (2017).
4. H. Tan, A. Jain, O. Voznyy, X. Lan, F. Arquer, J. Fan, R. Quintero-Bermudez and S. E., *Science.* **355**, 722 (2017).
5. K. Wang, L. Wu, L. Li, H. Yao, H. Qian and S. Yu, *Angew. Chem. Int. Ed.* . **55,** 8328 (2016).
6. W. Wei and Y. Hu, *Int. J. Energy Res.* **41**, 1063 (2017).
7. A. Slavney, R. Smaha, I. Smith, A. Jaffe, D. Umeyama and H. Karunadasa, *Inorg. Chem.* **56**, 46 (2017).
8. A. Swarnkar, R. Marshall, E. Sanehira, B. Chernomordik, D. Moore, J. Christians, T. Chakrabarti and J. Luther, *Science.* **354** 92 (2016).
9. Y. Tong, E. Bladt, M. Aygüler, A. Manzi, K. Milowska, V. Hintermayr, P. Docampo, S. Bals, A. Urban, L. Polavarapu and J. Feldmann, *Angew. Chem. Int. Ed.* **55**, 13887 (2016).
10. Z. Liu, S. Lee, W. Ma, Y. Bekenstein, X. Ye, S. Nguyen, S. Zhang, P. Yang and P. Alivisatos, *J. Am. Chem. Soc.* **139**, 5309 (2017).
11. F. Bella, G. Griffini, J. Correa-Baena, G. Saracco, M. Gratzel, A. Hagfeldt, S. Turri and C. Gerbaldi, *Science.* **354**, 203 (2016).
12. H. Tsai, W. Nie, J. Blancon, C. Stoumpos, R. Asadpour, B. Harutyunyan, A. Neukirch, R. Verduzco, J. Crochet, S. Tretiak, L. Pedesseau, J. Even, M. Alam, G. Gupta, J. Lou, P. Ajayan, M. Bedzyk and M. Kanatzidis, *Nature.* **536**, 312 (2016).
13. M. Saidaminov, J. Almutlaq, S. Sarmah, I. Dursun, A. Zhumekenov, R. Begum, J. Pan, N. Cho, O. Mohammed and O. Bakr, *ACS Energy Lett.* **1**, 840 (2016).
14. D. Chen, Z. Wan, X. Chen, Y. Yuan and J. Zhong, *J. Mater. Chem. C* **4**, 10646 (2016).
15. L. Protesescu, S. Yakunin, M. Bodnarchuk, F. Krieg, R. Caputo, C. Hendon, R. Yang, A. Walsh and M. Kovalenko, *Nano Lett.* **15**, 3692 (2015).
16. J. Sichert, Y. Tong, N. Mutz, M. Vollmer, S. Fischer, K. Milowska, R. Cortadella, B. Nickel, C. Cardenas-Daw, J. Stolarczyk, A. Urban and J. Feldmann, *Nano Lett.* **15**, 6521 (2015).
17. A. Binek, C. Hanusch, P. Docampo and T. Bein, *J. Phys. Chem. Lett.* **6**, 1249 (2015).
18. J. Xing, F. Yan, Y. Zhao, S. Chen, H. Yu, Q. Zhang, R. Zeng, H. Demir, X. Sun, A. Huan and Q. Xiong, *ACS Nano.* **10**, 6623 (2016).
19. H. Takaba, S. Kimura and M. K. Alam, *Chemical Physics.* **485**, 22 (2017).
20. E. M. Talbert, H. F. Zarick, A. Boulesbaa, N. Soetan, A. A. Puretzky, D. B. Geoheganb and R. Bardhan, *Nanoscale.* **9**, 11833 (2017).